SVU-International Journal of Engineering Sciences and Applications (2024) 5(2):275-282
Print ISSN: 2785-9967 | Online ISSN: 2735-4571
DOI: 10.21608/svusrc.2024.299456.1224

Augmentation of Jet Impingement Heat Transfer of Flat Plate via Humped Roughness Elements

Mustafa Abdelfattah (0000-0002-9754-8042) [1], **Mohamed A. Aziz** (0000-0001-9913-7282)[1], and **Hussein M. Maghrabie** (0000-0002-1016-1049) [2, ✉]

Abstract: This study explores the impact of humped roughness elements on heat transfer (HT) in the context of jet impingement. The roughness elements are widely employed across various industrial applications. Numerical simulation using the Re-Normalizations Group (RNG) k-ε turbulence model investigates the HT characteristics of a circular air jet directed onto a surface featuring a circular arrangement of humped roughness elements. The investigation covers a Reynolds number (***Re***) ranged from 7000 to 35000. The roughness elements are strategically positioned at distances relative-to-jet diameter (***s/d***) of 1.5, 2, 2.5, and 3. The study evaluates the local Temperature distribution (*T*), the average HT coefficient (h_{avg}) and its relative enhancement compared to a smooth plate ($h_{avg.r}$). The findings underscore a significant augmentation in HT performance with the humped configuration, showing $h_{avg.r}$ values reaching up to 1.2 times that of the smooth plate case. This enhancement is primarily attributed to the increased HT area and heightened turbulence intensity induced by the presence of the humped roughness elements, thereby facilitating more efficient HT rates.

Keywords: Humped elements, Heat transfer coefficient, Jet impingement, Roughness elements.

1 Introduction

Jet impingement heat transfer (JIHT) is a widely used method in numerous cooling applications [1]–[3]. To extend the operational lifetime of thermal components, it is necessary to achieve an efficient cooling process. One prevalent passive method involves altering the geometry and roughness of the target surface, often in combination with other modifications [4][5].

Received: 25 June 2024; Accepted: 24 August 2024
✉ Corresponding Author: **Hussein M. Maghrabie**,
E-mail: Hussein_mag@eng.svu.edu.eg, Hussein_mag@yahoo.com
[1] Department of Mechanical Engineering, Faculty of Engineering, Suez University, P.O. Box 43221, Suez, Egypt
[2] Department of Mechanical Engineering, Faculty of Engineering, South Valley University, P.O. Box 83523, Qena, Egypt

Using roughness parameters is common in heat transfer enhancement in many applications [6]–[8]. Previous studies have focused on several aspects of HT resulting from jet impingement. Attalla et al. [9] experimentally examined the average cooling rate of a target plate cooled by an impinging jet (IJ) with different degrees of roughness. The results indicated that increasing the roughness degree led to an improvement in the average Nusselt Number (Nu_{avg}). Wan et al. [10] examined the thermal characteristics of an air IJ on a surface roughened by various sizes of square pin-fins numerically. They reported that the highest HT rates were obtained by small pin-fins. Buzzard et al. [11] analyzed the thermal characteristics of IJs cooling a roughened target plate with a small-scale rectangle array of various patterns experimentally. They revealed that the roughness of the target plate augmented the ***Nu***.

Hadipour et al. [12] investigated the influence of micro-pins on fluid flow structure and HT characteristics by directing a round jet onto a target plate. They found that the pin-fins significantly affected the fluid flow, creating a sub-atmospheric pressure region downstream of the pins, which also improved the cooling rates. Secchi et al. [13] studied the influence of turbulent of a jet on the wall region for a smooth and rough target plate at a ***Re*** of 10000 numerically. It was observed that the outer layer velocity was not affected by the surface roughness. Zhang et al. [14] numerically investigated the flow structure and cooling rates on minor concentric ribs rough plate using Shear Stress Transport (SST) with transition model. For thermal analysis, the HT rates were better for small values of pitch-to-height ratios than that for higher values. Abdelfattah et al. [15] ensured that the small roughness elements that have curved edges enhanced the HT rates rather than other roughness elements shapes, principally the droplet shape. Rakhsha et al. [16] examined the impact of a circular arrangement of micro-pins on HT characteristics under both steady and pulsed flow conditions. The results revealed that employing a circular row of micro-pins enhanced Nu_{avg} up to 34%. Froissart et al. [17] studied the HT rates for a

smooth and rough-coned target plate cooled by an IJ. The surface induced a couple HT transition zones, which enhanced HT rates up to 11%. Forming the transition zone did not happen on the flat sheet nor the smooth sheet.

Lu et al. [18] studied the hydrodynamic and thermal characteristics of a target surface with micro-rectangular and pentahedron pins-fins cooled by arrays of jets. They studied the influence of pin-fin heights of 0.05, 0.2, and 0.4 of nozzle diameter. The results revealed that the best HT rates were made with the rectangular pin-fin. Tang et al. [19] numerically analyzed the HT rate of an IJ on a waved plate within a channel. Based on the control volume finite difference method, they applied the governing equations and the standard k-ε turbulence model. They found that when the wavelength of the corrugated plate gradually decreased, the Nu_{avg} significantly enhanced by 39.7% compared with that of the flat case. In addition, the optimum temperature distribution of the target plate occurred at a wave amplitude ratio of 0.2.

Hua et al. [20] examined the thermal characteristics of micro-pin fins on a heated surface with several natures. The results showed that at a constant ***Re***, the elliptical pin-fins achieved a higher ***Nu*** compared to other shapes. However, increasing the density of elliptical pin-fins resulted in reduced flow performance. Nagesha et al. [21] investigated the impact of V-grooves on the cooling rates of a target plate. They found that the grooves inhibited turbulence generation, and the trapped air between the grooves decreased the cooling rates. Xu et al. [22] numerically explored the impact of sinusoidal surface roughness on the ***Nu*** for air jet impingement. The results showed that the Nu_{avg} increased on the rough target plate, and the local temperatures (T) decreased due to fluid trapping in the valleys of the rough surface. Alenezi et al. [23] studied the influence of roughened target plate by ribs on cooling rates, considering the ribs height and ribs location numerically using a k-ε RNG turbulence model. It was noticed that the location of the rib in the stagnation point did not augment HT and the higher values of rib height were ineffective. Furthermore, they reported that the best HT rates were at x/d= 2 as it enhanced Nu_{avg} up to 15.6%.

Sharif and Ramirez [24] developed a method to simulate equal sand grain roughness for an IJ and compared various turbulence models. They observed that cooling rates increased with greater roughness height. Additionally, the roughness elements enhanced cooling rates by increasing the wetted area and turbulence intensity. Zhang et al. [25] examined the hydraulic and thermal characteristics of an IJ on a target surface with protrusions. They found that the cooling rates, both locally and on average, were higher for the protrusioned target plate compared to the smooth surface case. However, they observed that a separation region formed at the edge of the protrusions, which reduced the ***Nu***. Terekhov et al. [26] experimentally evaluated the thermal characteristics of IJ on a humped surface. The results showed that the ***Nu*** within the dimples was lower than that on a smooth surface. However, this reduction was completely compensated by the increased surface area of the humped surface.

Beitelmal et al. [27] studied the impact of surface roughness on the Nu_{avg} of air jet impingement experimentally. They compared a flat surface and a roughened surface by an array of circular with heights and bases of 0.5 mm. They found that the Nu_{avg} was augmented by up to 6%. Gau and Lee [28] examined the IJ cooling on a roughened plate by triangular ribs. They revealed that the HT over the triangular ribbed surface was better than that for the rectangular ribbed surface. Wei and Zu [29] investigated experimentally and numerically the enhancement in cooling rates and fluid flow structure for a double-wall system with IJs and pin-fins. They found that the ***Nu*** on the pin-fins was superior to that on the internal wall of the jet impingement plate. Hansen and Webb [30] investigated experimentally the impact of fin geometry on cooling a target plate compared to a smooth target plate under a circular air IJ. The results demonstrated that the Nu_{avg} for the rough surfaces decreased monotonically with increasing fin height. Chakroun et al. [31] examined the thermal characteristics of a circular IJ on a rough sheet experimentally. The local and average cooling rates for the rough impinging plate showed higher values than those for the smooth sheet case.

Ismail and Saha [32] studied experimentally the improvement of impinging air jet via perforated fins on the impinging plate. The results showed that the resistance reduced and the fin efficiency increased with growing the ***Re*** due to the perforation and decreased the rate of the consumed power. Matheswaran et al. [33] investigated the IJ on a flat plate roughened by arc obstacles. They reported an enhancement in exergetic efficiency by up to 56.8%. Furthermore, they observed that the roughened plate performed better at ***Re*** below 5900. Existing literature consistently supports the significant enhancement of HT rates using roughened plates. Additionally, they highlighted that smaller-scale roughness elements were more effective than larger elements. Li et al. [34] indicated that enhancing the h_{avg} was achieved by increasing both the height and width of the fin, which enlarged the impinged area. Furthermore, increasing the fin width augmented the convective area and mitigated flow resistance in the

passage. Additionally, they found that a combination of wider fins and ***Re*** increased HT rates.

Literature up-to-date indicated that the roughness enhanced the HT rates. Furthermore, these studies ensured that the roughness damped the velocity of the flow due to the drag force. So, this work investigates the effects of utilizing a single row of roughness elements and its location on the heat transfer of a flat plate. The current study investigates the effect of a single circular row of dimple roughness elements with a constant height of 500 µm and located away from the stagnation point at a ***s/d*** of 1.5, 2, 2.5, and 3. The HT rates of the roughened impinged plate are compared with the smooth plate at ***Re*** of 7000, 15000, 25000, and 35000. The paper is organized as follows: firstly, a literature of previous studies is presented and secondly, the study illustrates the problem description and makes the grid independence test and the governing equations are explained. Thirdly, the effect of the roughness elements will be investigated in the results section of local temperature distribution (T), average HT coefficient (h_{avg}), and average heat transfer coefficient ratio ($h_{avg,r}$).

2 Method and Materials

This study uses a CFD package FLUENT to solve the problem. K-ε RNG turbulence model is employed for closure since it is the most stable model that converges to residuals sooner than other turbulence models, which reduces the consumption time during the solution. As well, the standard wall function is applied as the wall treatment method. SIMPLE algorithm is used for pressure velocity coupling. Flow is considered as incompressible and constant properties.

2.1 Problem discerption

Fig. 1 illustrates a 3-D view of the problem and describes the boundaries. The study focuses on numerically evaluating the design of the target plate under impingement by an air jet. The effect of a target plate featuring a single circular row of humped roughness elements with that of a smooth flat surface is studied. A 2-D schematic of the geometry is shown in **Fig. 2**. The description outlines the setup and conditions for the numerical investigation of the target plate under impingement by an air jet. Key details include as follows:

Geometry and Dimensions: The ***s*** represents the distances from the roughness element center to stagnation point, d presents the nozzle diameter, and H displays the jet-to-target distance. **Table 1** shows the dimensions of the geometry parameters.

Table 1 Dimensions of the geometry parameters.

Parameter	value
d (mm)	12
s (mm)	18, 24, 30, and 36
H (mm)	24
D (mm)	78

- **Simplifications:** The study assumes steady flow and convective heat transfer. Flow through the plenum is neglected.
- **Boundary Conditions:** The target plate maintains a constant heat flux (***q***) of 2000 W/m². No-slip conditions apply to the nozzle wall and plate. Velocity inlets have uniform velocity distribution, with the air jet at T_j = 300 K. Turbulence intensity at the inlet is set to 5%. Ambient pressure is applied at the outlet.
- **Fluid Properties:** Air properties are assumed constant, i.e., density (ρ) of 1.225 kg/m^3, dynamic viscosity (υ) of 1.48x10^{-5} m^2/s, and thermal conductivity (λ) of 0.024 W/m.K.

This setup enables a focused numerical investigation into the HT characteristics of the target plate with and without roughness elements under impinging air jet conditions.

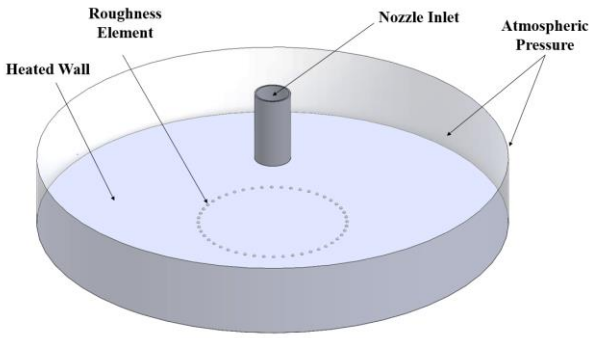

Fig. 1. A 3-D view of the problem.

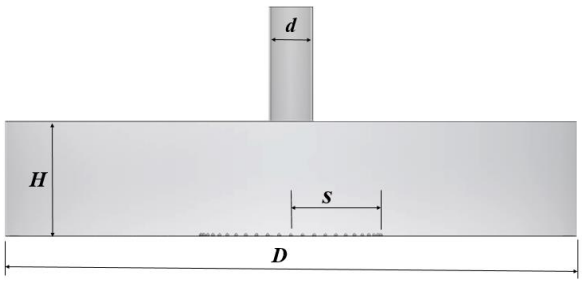

Fig. 2. A 2-D sketch of the problem.

2.2. Validation of the numerical model

Fig. 3 shows the effect of ***Re*** on h_{avg} at ***s/d*** =3 for roughness elements and compares the results with the experimental data of Beitelmal et al. [27] who studied the effects of surface roughness on the average heat transfer of an impinging air free jet. The literature data used dimples as roughness elements at ***s/d*** of 3 for ***Re*** in the range of 10000-37500. It is noticed that the present study and the literature have matched values of h_{avg}. The evaluation of the work validation is based on statistical parameters. the values of the mean absolute percentage error, standard deviation, mean square error and *R*-squared are 4.7%, 3.7%, 36.2, and 0.978, respectively.

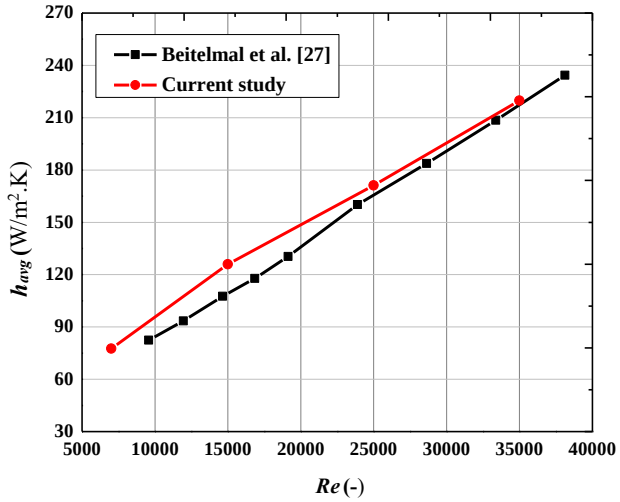

Fig. 3. Comparison between the current work and Beitelmal et al. [27] based on the results of h_{avg}.

2.3 Grid independence

Fig. 4 shows the h_{avg} on the target surface for a roughened case at ***Re*** of 7000 for each mesh size. The results show that an independent on the number of mesh elements higher than 1,326,594 elements. As well, the study considers the grid sizes of 0.151x10^6, 0.51x10^6, 0.92 x10^6, 1.32x10^6, and 3.06 x10^6. By increasing the grid size from 1,326,594 to 3,056,740 elements, the consistent results reach an error of 0.003%. The convergence residuals are 10^{-6} for energy and 10^{-5} for other parameters. The minimum element size of 10^{-4} mm, 5 degrees' curvature normal angle, and 1.1 growth rate are selected in order to satisfy high-quality mesh and y^+<1 condition for the RNG k–ε turbulence model.

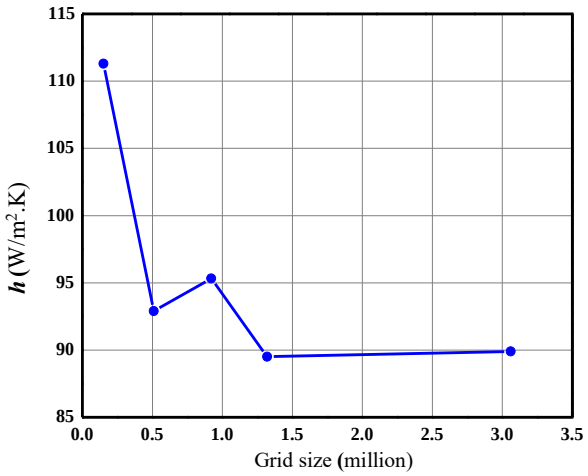

Fig. 4 Grid sensitivity analysis.

2.4 Governing equations

The numerical study was conducted to determine whether any of two-equation turbulence models can help in heat transfer prediction results. In this study, the flow is assumed to be three-dimensional, incompressible, statistically steady and turbulent. The effect of buoyancy is neglected. the continuity, momentum, and energy equations are solved in this work as follows [35]:

Continuity equation:

$$\frac{\partial \overline{u_i}}{\partial x_i} = 0 \quad (1)$$

Momentum equation:

$$\rho \frac{\partial}{\partial x_i}(\overline{u_i}\overline{u_j}) = -\frac{\partial \overline{p}}{\partial x_i} + \frac{\partial}{\partial x_j}\left\{\mu\left(\frac{\partial \overline{u_i}}{\partial x_j} + \frac{\partial \overline{u_j}}{\partial x_i}\right) - \rho\overline{u_i'u_j'}\right\} \quad (2)$$

Energy equation:

$$\rho\overline{u_j}\frac{\partial \overline{T}}{\partial x_j} = \frac{\partial}{\partial x_i}\left\{\frac{\lambda}{C_p}\frac{\partial \overline{T}}{\partial x_j} - \rho\overline{u_j'T'}\right\} \quad (3)$$

where u_p represents velocity component in corresponding direction, T is the temperature, p is the pressure, u_i' is the fluctuating velocity component, and T' is the fluctuating temperature.

The k and ε transport equations are [36]:

$$\frac{\partial}{\partial t}(\rho k) + \frac{\partial}{\partial x_i}(\rho k u_i) = \frac{\partial}{\partial x_j}\left(\frac{\mu_t}{\sigma_k}\frac{\partial k}{\partial x_j}\right) + 2\mu_t E_{ij}E_{ij} - \rho\varepsilon \quad (4)$$

$$\frac{\partial}{\partial t}(\rho\varepsilon) + \frac{\partial}{\partial x_i}(\rho\varepsilon u_i) = \frac{\partial}{\partial x_j}\left(\frac{\mu_t}{\sigma_\varepsilon}\frac{\partial \varepsilon}{\partial x_j}\right) + C_{1\varepsilon}\frac{\varepsilon}{k}E_{ij}E_{ij} - C_{2\varepsilon}\rho\frac{\varepsilon^2}{k} \quad (5)$$

where E_{ij} represents component of rate of deformation and μ_t represents the eddy viscosity. σ_k, σ_ε, $C_{1\varepsilon}$, and $C_{2\varepsilon}$ are constants.

The Reynolds number (Re) and Nusselt number (Nu) are defined as follows [37]:

$$Re = \frac{\rho U d}{\mu} \quad (6)$$

$$h = \frac{q}{T_s - T_j} \quad (7)$$

3. Results and Discussion

The effect of using the humped roughness elements on JIHT is studied numerically and compared with that of the smooth case. The study examines the effect of the ***Re*** and the ***s/d*** on the h_{avg} and the average heat transfer coefficient ratio ($h_{avg.r}$).

3.1 Local Temperature

Fig. 5 illustrates the local temperature distribution on the heated surface for the smooth and roughened surfaces of $s/d = 2$ and a ***Re*** of 7000, 15000, 25000, and 35000. The dark colors refer to low temperature and light colors refers to high temperature. It is noticed that increasing Reynolds number decreases the temperature all over the plate. Additionally, the temperature increases in the radial directions outwards the stagnation region. As well, it is observed that the local temperatures of the roughened plate are lower than that of the smooth plate. Furthermore, the lowest temperature of the roughened plate is obtained at the location of the roughness elements.

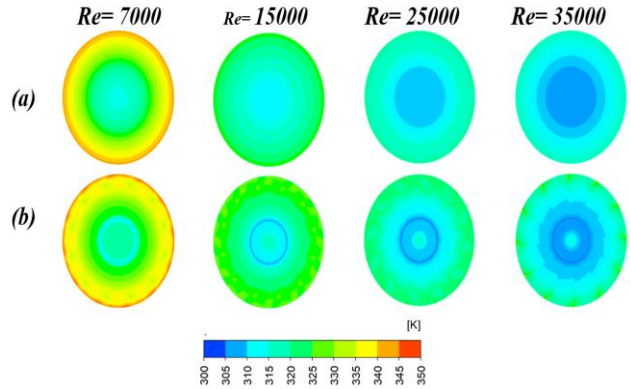

Fig. 5 Local Temperature distribution on the target plate for (a) smooth plate (b) roughened plate.

3.2 Average heat transfer coefficient (h_{avg})

3.2.1 Effect of Reynolds number (***Re***)

Fig. 6 represents the impact of jet ***Re*** on h_{avg} for smooth and roughened surfaces at ***s/d*** of 1.5, 2, 2.5, and 3. At all values of ***s/d***, the h_{avg} increases significantly with increasing the jet ***Re*** due to the rise of the flow momentum and the turbulence. The h_{avg} for the smooth flat plate equals 80.2, 119.4, 157.96, and 196.88 W/m^2.K for a ***Re*** of 7000, 15000, 25000, and 35000, respectively.

At ***s/d*** of 1.5 and 2, the h_{avg} of the roughened is better than that of the smooth case since the roughness elements increased the wetted area and the turbulence intensity. At ***Re*** of 35000 and a ***s/d*** of 1.5, h_{avg} equals 236.64 and 196.88 W/m^2.K for roughened and smooth target plate, respectively. The enhancement that occurs at roughened plate cases is a result of increasing the wetted area, which increases the cooling rates. Additionally, the increase in HT rates is a result of the increase in flow velocity at the passages between the elements and the increase in turbulence intensity [38]. In addition, it is noticed that the enhancement of h_{avg} is growing by an increase of ***Re*** because the growth in HT rates at a ***Re*** of 35000 is higher than that at a ***Re*** of 7000. This result is due to the high thickness of the hydraulic boundary layer and the significant impact of the drag force.

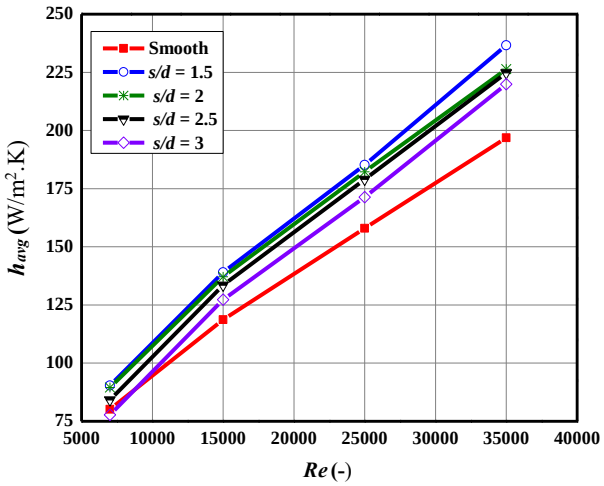

Fig. 6 Effect of ***Re*** on h_{avg} for smooth and roughened plate at different locations.

3.2.2 Effect of roughness elements location (***s/d***)

The influence of ***s/d*** on the h_{avg} at a jet ***Re*** of 7000, 15000, 25000, and 35000 is shown in **Fig. 7**. For all values of ***Re*** of humped shapes, the increase in ***s/d***, decreases the h_{avg} on the target plate. For the roughened surface at of 35000, the h_{avg} equals 236.6, 226.44, 224.8, and 219.85 for a ***s/d*** of 1.5, 2, 2.5, and 3, respectively. The decrease in the cooling rates with increasing the ***s/d*** is due to the growth of the thickness

of the hydraulic boundary layers at higher values of ***s/d***. Moreover, the velocity of the flow is damped into the radial direction outwards the stagnation region location of the roughness elements due to the drag force that resulted from applying the no slip condition on the wall.

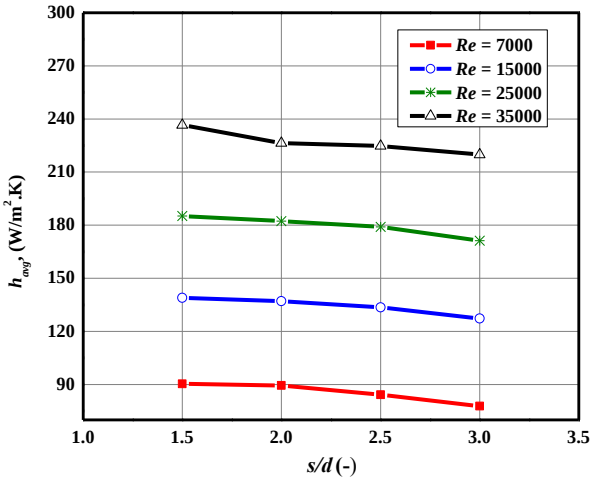

Fig. 7. Effect of ***s/d*** on h_{avg} at different values of ***Re*** for the roughened surface.

3.3 Average heat transfer coefficient ratio ($h_{avg.r}$)

The $h_{avg.r}$ is the ratio between the heat transfer coefficient of the roughened surface ($h_{avg.rough}$) to the average heat transfer coefficient on the smooth ($h_{avg.smooth}$).

$$h_{avg.r} = \frac{h_{avg.rough}}{h_{avg.smooth}} \quad (8)$$

3.3.1 Effect of Reynolds number (***Re***)

The $h_{avg.r}$ versus ***Re*** for different values of ***s/d*** is represented in **Fig. 8**. For all values of roughness element location (***s/d***), $h_{avg.r}$ increases by increasing ***Re***. The results show that at ***s/d*** =2, the $h_{avg.r}$ equals 1.12, 1.16, 1.15, and 1.16 for a ***Re*** of 7000, 15000, 25000, and 35000, respectively.

3.3.2 Effect of roughness elements location (***s/d***)

The $h_{avg.r}$ versus ***s/d*** for different values of ***Re*** is represented **Fig. 9.** In addition, the growing in ***s/d*** reduces the h_{avg}. At a ***Re*** of 25000, the $h_{avg.r}$ equals 1.17, 1.15, 1.13, and 1.08 for a ***s/d*** of 1.5, 2, 2.5, and 3, respectively. The highest value of $h_{avg.r}$ is noticed to be at ***s/d*** = 1.5 for all values of ***Re*** because the hydraulic boundary layer thickness is low at the low ***s/d*** distances.

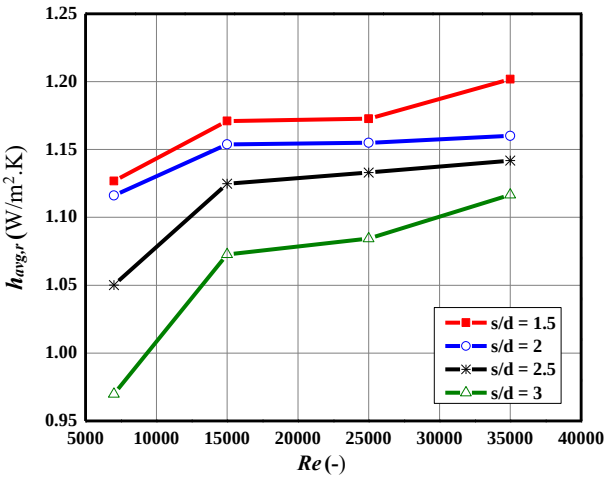

Fig. 8. Effect of ***Re*** on $h_{avg.r}$ at different values of ***s/d***.

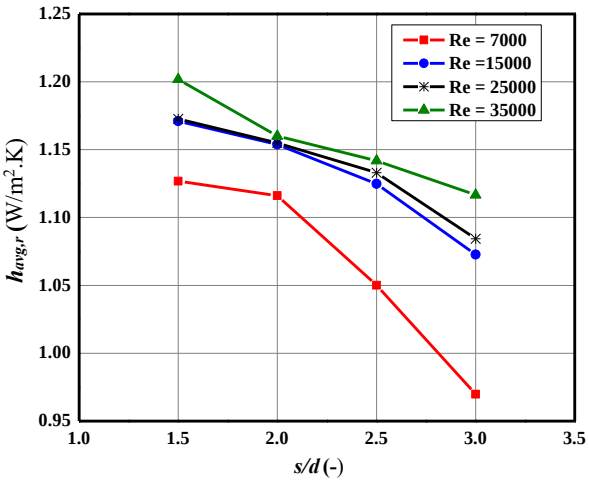

Fig. 9. Effect of ***s/d*** on $h_{avg.r}$ at different values of ***Re***.

Nomenclature

C_p	specific heat, (J/kg)
d	jet diameter, (m)
D	diameter of flat plate, (m)
H	jet-to-plate distance, (m)
h	convection heat transfer coefficient, (W/m^2.K)
K	turbulent kinetic energy
Nu	Nusselt number, (-)
p	static pressure, (Pa)
q	heat flux, (W/m^2)
Re	Reynolds number, (-)
s	roughness element location, (m)
T	temperature, (K)
U	jet velocity, (m/s)

Greek Letters

μ	dynamic viscosity, (N.s/m^2)
ε	rate of dissipation of turbulent kinetic energy

σ_ε	dissipated turbulence energy
σ_k	Prandtl number for turbulence energy
ρ	air density, (kg/m^3)
λ	air thermal conductivity, (W/m.K)
Subscripts	
avg	average
j	jet
r	ratio
Abbreviations	
HT	Heat Transfer
IJ	Impinging Jet
JIHT	Jet Impingement Heat Transfer
RNG	Re-Normalizations Group
SST	Shear Stress Transport

4 Conclusions

The average HT rates of a target plate roughened by a circular row of humped roughness elements with height of 500 μm were studied numerically. Smooth flat plate and roughened one using impinged by an air jet were examined. The impact of ***Re*** and ***s/d*** were investigated. The results of the study are highlighted as follows:

- Using a row of roughness elements surrounding the stagnation region on the plate enhanced the h_{avg} and the cooling rates. This due to the increase of the wetted area of the target surface as a result of using roughness elements.
- The existence of the roughness elements enhances the reduction of local temperature on the target plate particularly at the location of the roughness elements.
- Increasing ***Re*** enhanced the h_{avg} for smooth target plate as well as roughened target plate because of increasing the momentum of the flow. At a ***s/d*** of 1.5 and 2, the h_{avg} of the roughened is better than that of the smooth case. At a ***Re*** of 35000 and a ***s/d*** of 1.5, the h_{avg} equals 236.64, and 196.88 W/m^2.K for roughened and smooth plates, respectively.
- Increasing ***s/d*** decreased the h_{avg} for all values of ***Re*** as a result of the growth of the hydraulic boundary layer. For the roughened surface at of 35000, the h_{avg} equals 236.6, 226.44, 224.8, and 219.85 W/m^2.K for a ***s/d*** of 1.5, 2, 2.5, and 3, respectively.
- Increasing ***Re*** enhanced the $h_{avg.r}$ for roughened target plate. At ***s/d*** =2, the $h_{avg.r}$ equals 1.12, 1.16, 1.15, and 1.16 for a ***Re*** of 7000, 15000, 25000, and 35000, respectively.
- Increasing ***s/d*** decreased the $h_{avg.r}$ for all ***Re*** values. At ***Re*** of 25000, the $h_{avg.r}$ equals 1.17, 1.15, 1.13, and 1.08 for a ***s/d*** of 1.5, 2, 2.5, and 3, respectively.

References

[1] A. A. El –Wafa, H. M. Maghrabie, M. Attalla, and A. N. Shmroukh, "Heat transfer uniformity of a flat plate impinged by movable double nozzles: An experimental implementation," *Appl. Therm. Eng.*, vol. 247, p. 123016, 2024., doi.org/10.1016/j.applthermaleng.2024.123016

[2] S. D. Barewar *et al.*, "Optimization of jet impingement heat transfer : A review on advanced techniques and parameters," *Therm. Sci. Eng. Prog.*, vol. 39, p. 101697, 2023, doi: 10.1016/j.tsep.2023.101697.

[3] H. M. Maghrabie, M. Attalla, and M. Abdelfattah, "Heat Transfer Intensification of a Confined Impinging Air Jet Via a Guiding Baffle," *ASME J. Heat Mass Transf.*, vol. 145, no. 7, p. 072301, 2023, doi: 10.1115/1.4057051.

[4] R. J. Talapati and V. V. Katti, "Influence of turbulator under the detached rib on heat transfer study of air jet impinging on a flat surface," *Int. J. Therm. Sci.*, vol. 184, p. 107946, 2023, doi: 10.1016/j.ijthermalsci.2022.107946.

[5] H. M. Maghrabie, "Heat transfer intensification of jet impingement using exciting jets - A comprehensive review," *Renew. Sustain. Energy Rev.*, vol. 139, p. 110684, 2021, doi: 10.1016/j.rser.2020.110684.

[6] M. Attalla and H. M. Maghrabie, "An experimental study on heat transfer and fluid flow of rough plate heat exchanger using Al_2O_3/water nanofluid," *Exp. Heat Transf.*, vol. 33, no. 3, pp. 261–281, 2019, doi: 10.1080/08916152.2019.1625469.

[7] M. Attalla and H. M. Maghrabie, "Investigation of effectiveness and pumping power of plate heat exchanger with rough surface," *Chem. Eng. Sci.*, vol. 211, p. 115277, 2020, doi: 10.1016/j.ces.2019.115277.

[8] M. Attalla, H. M. Maghrabie, and E. Specht, "An experimental investigation on fluid flow and heat transfer of rough mini-channel with rectangular cross section," *Exp. Therm. Fluid Sci.*, vol. 75, pp. 199–210, 2016, doi: 10.1016/j.expthermflusci.2016.01.019.

[9] M. Attalla, A. A. Abdel Samee, and N. N. Salem, "Experimental investigation of heat transfer of impinging jet on a roughened plate by a micro cubic shape," *Exp. Heat Transf.*, vol. 33, no. 3, pp. 210–225, 2020, doi: 10.1080/08916152.2019.1614113.

[10] C. Wan, Y. Rao, and X. Zhang, "Numerical Investigation of Impingement Heat Transfer on a Flat and Square Pin-Fin Roughened Plates," in *In Turbo Expo: Power for Land, Sea, and Air*, 2013, vol. 55140, p. V03AT12A016.

[11] W. C. Buzzard, Z. Ren, P. M. Ligrani, C. Nakamata, and S. Ueguchi, "Influences of target surface small-scale rectangle roughness on impingement jet array heat transfer," *Int. J. Heat Mass Transf.*, vol. 110, pp. 805–816, 2017, doi: 10.1016/j.ijheatmasstransfer.2017.03.061.

[12] A. Hadipour, M. Rajabi Zargarabadi, and M. Dehghan, "Effect of micro-pin characteristics on flow and heat transfer by a circular jet impinging to the flat surface," *J. Therm. Anal. Calorim.*, vol. 140, no. 3, pp. 943–951, 2020, doi: 10.1007/s10973-019-09232-2.

[13] F. Secchi, D. Gatti, and B. Frohnapfel, "The Wall-Jet Region of a Turbulent Jet Impinging on Smooth and Rough Plates," *Flow, Turbul. Combust.*, vol. 110, no. 2, pp. 275–299, 2023, doi: 10.1007/s10494-022-00387-x.

[14] G. Zhang, H. Huang, T. Sun, and Z. Zhang, "Flow structures and heat transfer on small-scale concentric ribs rough surface for confined turbulent jet impingement,"

Int. Commun. Heat Mass Transf., vol. 137, p. 106218, 2022, doi: 10.1016/j.icheatmasstransfer.2022.106218.

[15] M. Abdelfattah, M. A. Aziz, and H. M. Maghrabie, "Numerical analysis of heat transfer and fluid flow structures of jet impingement on a flat plate with different shapes of roughness elements," *Numer. Heat Transf. Part A Appl.*, pp. 1–26, 2024, doi: 10.1080/10407782.2024.2379032.

[16] S. Rakhsha, M. Rajabi Zargarabadi, and S. Saedodin, "Experimental and numerical study of flow and heat transfer from a pulsed jet impinging on a pinned surface," *Exp. Heat Transf.*, vol. 34, no. 4, pp. 376–391, 2021, doi: 10.1080/08916152.2020.1755388.

[17] M. Froissart, P. Ziółkowski, W. Dudda, and J. Badur, "Heat exchange enhancement of jet impingement cooling with the novel humped-cone heat sink," *Case Stud. Therm. Eng.*, vol. 28, p. 101445, 2021, doi: 10.1016/j.csite.2021.101445.

[18] X. Lu, W. Li, X. Li, J. Ren, H. Jiang, and P. Ligrani, "Flow and heat transfer characteristics of micro pin-fins under jet impingement arrays," *Int. J. Heat Mass Transf.*, vol. 143, p. 118416, 2019, doi: 10.1016/j.ijheatmasstransfer.2019.07.066.

[19] Z. Tang, C. Yin, R. Sun, and J. Cheng, "Study on the flow and heat transfer of a nanofluid hybrid jet impinging on a corrugated microchannel heat sink," *Int. J. Therm. Sci.*, vol. 194. p. 108590, 2023. doi: 10.1016/j.ijthermalsci.2023.108590.

[20] J. Hua, G. Li, X. Zhao, and Q. Li, "Experimental study on thermal performance of micro pin fin heat sinks with various shapes," *Heat Mass Transf.*, vol. 53, pp. 1093–1104, 2017, doi: 10.1007/s00231-016-1880-8.

[21] K. Nagesha, K. Srinivasan, and T. Sundararajan, "Enhancement of jet impingement heat transfer using surface roughness elements at different heat inputs," *Exp. Therm. Fluid Sci.*, vol. 112, p. 109995, 2020, doi: 10.1016/j.expthermflusci.2019.109995.

[22] P. Xu, A. P. Sasmito, S. Qiu, A. S. Mujumdar, L. Xu, and L. Geng, "Heat transfer and entropy generation in air jet impingement on a model rough surface," *Int. Commun. Heat Mass Transf.*, vol. 72, pp. 48–56, 2016, doi: 10.1016/j.icheatmasstransfer.2016.01.007.

[23] A. H. Alenezi, A. Almutairi, H. M. Alhajeri, A. Addali, and A. A. A. Gamil, "Flow structure and heat transfer of jet impingement on a rib-roughened flat plate," *Energies*, vol. 11, no. 6, p. 1550, 2018, doi: 10.3390/en11061550.

[24] M. A. R. Sharif and N. M. Ramirez, "Surface roughness effects on the heat transfer due to turbulent round jet impingement on convex hemispherical surfaces," *Appl. Therm. Eng.*, vol. 51, no. 1–2, pp. 1026–1037, 2013, doi: 10.1016/j.applthermaleng.2012.10.015.

[25] D. Zhang, H. Qu, J. Lan, J. Chen, and Y. Xie, "Flow and heat transfer characteristics of single jet impinging on protrusioned surface," *Int. J. Heat Mass Transf.*, vol. 58, no. 1–2, pp. 18–28, 2013, doi: 10.1016/j.ijheatmasstransfer.2012.11.019.

[26] V. I. Terekhov, S. V. Kalinina, Y. M. Mshvidobadze, and K. A. Sharov, "Impingement of an impact jet onto a spherical cavity. Flow structure and heat transfer," *Int. J. Heat Mass Transf.*, vol. 52, no. 11–12, pp. 2498–2506, 2009, doi: 10.1016/j.ijheatmasstransfer.2009.01.018.

[27] A. H. Beitelmal, M. A. Saad, and C. D. Patel, "Effects of surface roughness on the average heat transfer of an impinging air jet," *Int. Commun. Heat Mass Transf.*, vol. 27, no. 1, pp. 1–12, 2000, doi: 10.1016/S0735-1933(00)00079-8.

[28] C. Gau and I. C. Lee, "Flow and impingement cooling heat transfer along triangular rib-roughened walls," *Int. J. Heat Mass Transf.*, vol. 43, no. 24, pp. 4405–4418, 2000, doi: 10.1016/S0017-9310(00)00064-8.

[29] H. Wei and Y. Zu, "Experimental and numerical studies on the enhanced heat transfer performance and the flow resistance characteristics of the double-wall cooling structure with jet impingement holes and pin fins," *Int. J. Therm. Sci.*, vol. 186, p. 108109, 2023, doi: 10.1016/j.ijthermalsci.2022.108109.

[30] L. G. Hansen and B. W. Webb, "Air jet impingement heat transfer from modified surfaces," *Int. J. Heat Mass Transf.*, vol. 36, no. 4, pp. 989–997, 1993, doi: 10.1016/S0017-9310(05)80283-2.

[31] W. M. Chakroun, S. F. Al-Fahed, and A. A. Abdel-Rehman, "Heat transfer augmentation for air jet impinged on a rough surface," *Appl. Therm. Eng.*, vol. 18, no. 12, pp. 1225–1241, 1998, doi: 10.1016/S1359-4311(97)00100-2.

[32] M. F. Ismail and S. C. Saha, "Enhancement of confined air jet impingement heat transfer using perforated pin-fin heat sinks," in *Application of Thermo-fluid Processes in Energy Systems: Key Issues and Recent Developments for a Sustainable Future*, 2018, pp. 231–243. doi: 10.1007/978-981-10-0697-5_10.

[33] M. M. Matheswaran, T. V. Arjunan, and D. Somasundaram, "Analytical investigation of exergetic performance on jet impingement solar air heater with multiple arc protrusion obstacles," *J. Therm. Anal. Calorim.*, vol. 137, pp. 253–266, 2019, doi: 10.1007/s10973-018-7926-z.

[34] Li, H.Yi, S. M. Chao, and G. Tsai, "Thermal performance measurement of heat sinks with confined impinging jet by infrared thermography," *Int. J. Heat Mass Transf.*, vol. 48, no. 25–26, pp. 5386–5394, 2005, doi: 10.1016/j.ijheatmasstransfer.2005.07.007.

[35] S. V. Patankar, *Numerical Heat Transfer and Fluid Flow*. CRC press, 2018.

[36] W. Versteeg, Henk Kaarle; Malalasekera, *An introduction to Computational Fluid Dynamics: The Finite Volume Method*, Second. Pearson Education, 2007.

[37] R. You, J. Che, H. Li, and Z. Tao, "Flow and heat transfer in rotating smooth and ribbed multi-channel double-wall structure with multiple-jet impingement cooling," *Therm. Sci. Eng. Prog.*, vol. 42, p. 101917, 2023, doi: 10.1016/j.tsep.2023.101917.

[38] V. N. M.K. Chyu, "Heat transfer on the base surface of three dimensional protruding elements," *Int. J. Heat Mass Tran.*, vol. 39, no. 14, pp. 2925–2935., 1996, doi: https://doi.org/10.1016/0017-9310(95)00381-9.